

Low-energy collisions between electrons and BeD⁺

S. Niyonzima^{1,2}, N. Pop³, F. Iacob⁴, Å. Larson⁵, A.E. Orel⁶, J. Zs Mezei^{2,7,8}, K. Chakrabarti⁹, V. Laporta^{2,10}, K. Hassouni⁷, D. Benredjem¹¹, A. Bultel¹², J. Tennyson¹⁰, D. Reiter¹³, and I. F. Schneider^{2,11*}

¹*Dépt. de Physique, Faculté des Sciences, Université du Burundi, B.P. 2700 Bujumbura, Burundi*

²*LOMC CNRS–Université du Havre–Normandie Université, 76058 Le Havre, France*

³*Dept. of Fundamental of Physics for Engineers,*

Politehnica University Timisoara, 300223 Timisoara, Romania

⁴*Dept. of Physics, West University of Timișoara, 300223 Timișoara, Romania*

⁵*Dept. of Physics, Stockholm University, AlbaNova University Center, 106 91 Stockholm, Sweden*

⁶*Dept. of Chemical Engineering, University of California, Davis, California 95616, USA*

⁷*LSPM, CNRS–Université Paris 13–USPC, 93430 Villetaneuse, France*

⁸*HUN-REN Institute for Nuclear Research (ATOMKI), H-4001 Debrecen, Hungary*

⁹*Dept. of Mathematics, Scottish Church College, Calcutta 700 006, India*

¹⁰*Dept. of Physics and Astronomy, University College London, WC1E 6BT London, UK*

¹¹*LAC, CNRS–Université Paris-Sud–ENS Cachan–Université Paris-Saclay, 91405 Orsay, France*

¹²*CORIA CNRS–Université de Rouen–Université Normandie, F-76801 Saint-Etienne du Rowray, France and*

¹³*IEK, Forschungszentrum Jülich GmbH Association EURATOM-FZJ,*

Partner in Trilateral Cluster, 52425 Jülich, Germany

(Dated: May 31, 2024)

Multichannel quantum defect theory is applied in the treatment of the dissociative recombination and vibrational excitation processes for the BeD⁺ ion in the twenty four vibrational levels of its ground electronic state ($X^1\Sigma^+, v_r^+ = 0 \dots 23$). Three electronic symmetries of BeD^{**} states ($^2\Pi$, $^2\Sigma^+$, and $^2\Delta$), are considered in the calculation of cross sections and the corresponding rate coefficients. The incident electron energy range is 10^{-5} –2.7 eV and the electron temperature range is 100–5000 K. The vibrational dependence of these collisional processes is highlighted. The resulting data are useful in magnetic confinement fusion edge plasma modelling and spectroscopy, in devices with beryllium based main chamber materials, such as ITER and JET, and operating with the deuterium-tritium fuel mix. An extensive rate coefficients database is presented in graphical form and also by analytic fit functions whose parameters are tabulated in the supplementary material.

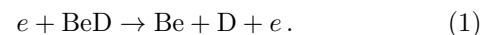
PACS numbers: 33.80.-b, 42.50. Hz

I. INTRODUCTION

The International Thermonuclear Experimental Reactor (ITER) is aimed at demonstrating the scientific and technological feasibility of fusion power [1]. It is now widely accepted by the fusion community that some form of controlled thermonuclear reactor, capable of producing a useful amount of electrical power, will be built-in the not-too-distant future. To obtain tenfold power multiplication in a controlled fusion process, at a power level greater than 500 MW and during pulses of 10 min or longer, exothermic reactions involving light nuclei, those between the hydrogen isotopes, are by far the most probable and efficient. The Joint European Torus (JET), in operation since 1983, has been persistently upgraded, most recently to become an ITER-like wall. It's the largest and most powerful tokamak in the world capable of operating with the deuterium-tritium fuel mix. One of the main improvements of JET was to equip the vessel with a first wall material combination comprising beryllium (Be) in the main chamber and tungsten (W) in the divertor [2–4]. These plasma facing components are expected to improve the machine conditioning, impact on operational space and energy confinement. The installa-

tion of Be and W in the main chamber wall of JET is aimed at studying the impurity evolution and material migration under plasma and material conditions relevant for ITER [5]. The selection of beryllium in the main chamber wall is explained by its operational flexibility anticipated for a low-Z main wall [6], its low-fuel retention and excellent oxygen getter property, confirmed experimentally [4, 7]. In tokamaks, material erosion limits the lifetime of plasma-facing components, while in the edge and divertor regions of fusion reactors, plasma-wall interactions generate new molecular species, this formation of impurities being allowed by the relatively low-temperatures of this region of the fusion plasma. Moreover, due to the strong chemical affinity of beryllium and tungsten to oxygen, those surfaces will be oxidized [8].

In JET, the formation of BeD as well as the presence of Be, Be⁺, BeD⁺, BeT⁺ and other impurities into the plasma are clearly described in [2, 10] and experimentally confirmed by spectroscopic methods [2–4, 11, 12, 14]. Be erosion as well as its continuous deposition towards the divertor is intrinsic to plasma operation due to the relatively high chemically assisted physical sputtering yield of Be *via* the radical BeD molecule [4] which dissociates by the reactions [3]:



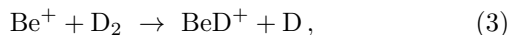
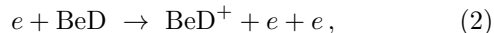
Though deuterium ion bombardment of Be targets may cause the formation of the stable BeD₂ molecule near the main chamber, there is no spectroscopic access to

*ioan.schneider@univ-lehavre.fr

the BeD₂ molecule released by chemically assisted physical sputtering of Be wall [3, 12]. Furthermore, retention of fuel elements by implantation in Be is expected to be saturated quickly due to the narrow interaction zone [7]. With the full W divertor installed in JET, all Be ions flowing into the inner divertor [11] are originated primarily in the main chamber during diverted plasma operation. Finally, the main physics mechanism responsible for the fuel retention under the Be wall conditions in the JET experiments is co-deposition of fuel in Be co-deposits [7]. The rate of fuel retention with the ion flux to the main plasma facing components in both the divertor and main chamber is increased by co-deposition of fuel atoms with Be [6, 14]. This information is in line with the measured spectral line emission of BeII (Be⁺) influx [4, 12] from the main chamber into the inner divertor whose plasma-facing surfaces are a net deposition zone [11].

In tokamaks with Be/W environment, all studies leading to physics understanding of beryllium migration and connecting the lifetime of the first wall components under erosion, with tokamak safety, in relation to the temporal behaviour of each fraction contribution to the long-term retention. The erosion mechanism itself is not studied in this work, but we are interested in providing data to support diagnosing beryllium in the fusion plasma. Moreover, in JET equipped with Be/W wall environment and operating with deuterium-tritium fuel mix, the rate of Be erosion is measured by spectroscopy of all the states of the atoms and molecules, so primarily of Be, Be⁺, Be₂⁺, BeD, BeD⁺, BeT, BeT⁺, BeD₂, BeDT, BeT₂, BeD₂⁺, BeDT⁺ and BeT₂⁺. Several observations of Be erosion by optical emission spectroscopy of various transitions of Be (at 457 nm) [2, 3], Be⁺ (at 527 nm and 436nm) [3] and the A²Σ⁺ → X²Σ⁺ band emission of BeD (band head at 497-500 nm) [12, 13] under different plasma conditions and surface temperatures, have been carried out successfully in laboratories and JET experiments.

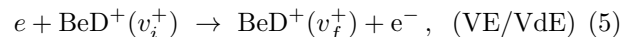
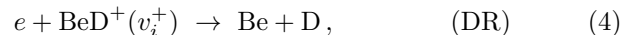
As shown in Ref [2], BeD and BeD⁺ are the only beryllium hydride molecules released in the plasma. Even though BeD⁺ is expected to be stable in the JET divertor plasma [15], being formed through the reactions [3, 12],



its A¹Σ⁺ → X¹Σ⁺ band emission in visible and ultraviolet range is not observable, probably due to its weak intensities [15, 16]. Be is the main and dominant intrinsic impurity in limited and diverted plasmas with the JET. Those impurities hugely influence the low temperature edge and divertor plasma behaviour in which electrons and ions originating from the core plasma are cooled by radiation and charge exchange processes till below 1 eV [1, 17, 18]. All molecular species in these regions undergo many collisions in particular those between electrons and molecular ions are of crucial importance [17]. The electron-impact processes of vibrationally excited BeD⁺ play a key role in the reaction kinetics of low-temperature plasmas in general, and particularly also in certain cold regions of fusion reactor relevant (*e.g.*

the divertor) plasmas. Hence, modelling and diagnosing these varied plasma environments require accurate, reliable cross-sections and rate coefficients for interactions of these molecular ions with electrons [19, 20] which produce simpler species, most of which being unsuitable for visible spectroscopy. The present complete database of cross-sections and rate coefficients for electron-impact collision processes coupled to the availability of absolutely calibrated spectroscopic emission from this molecular ion provides a way to characterise also the BeD⁺ formation rates in the edge and divertor plasma of fusion devices.

This work is a part of a series of papers [9, 10, 21–23] devoted to the study of electron-impact processes in fusion devices with beryllium-based main chamber materials. This series was dedicated to the BeH⁺ and BeH species, but they also contained preliminary studies of the isotopic effects. According to Figure 5 from [9] and Figure 11 from [21], these effects are quite notable, and this has pushed us to address it in a systematic and exhaustive manner. In this article, we present reactive collisions cross sections and rate coefficients between electrons and the BeD⁺ molecular ion in all vibrational states, relevant for the divertor and edge plasma kinetics of JET and ITER. In collision with electrons the BeD⁺ ion undergoes several processes, in particular dissociative recombination (DR) and vibrational-excitation/de-excitation (VE/VdE), respectively [24, 25]:



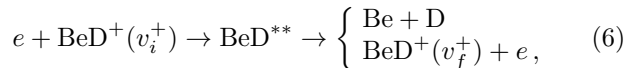
where $v_i^+(v_f^+)$ denote the initial(final) vibrational level of the cation. At an energy exceeding the dissociation energy of BeH⁺ (calculated to be 2.68 eV, see below) also the process of dissociative excitation sets it. It is not considered in the present paper.

The manuscript is organized as follows: In Section II, we briefly review the theoretical method used to calculate the cross sections and the corresponding rate coefficients; Section III presents Maxwellian isotropic rate coefficients computed for the DR, VE and VdE processes. These rate coefficients have been fitted with a modified Arrhenius law. Section IV contains the final remarks concluding the paper.

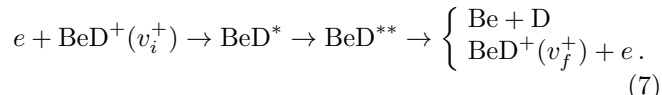
II. BRIEF DESCRIPTION OF THE THEORETICAL APPROACH OF THE DYNAMICS

In the present paper, we used the Multichannel Quantum Defect Theory (MQDT)-type approach [26] to study the vibrational resolved reactive collisions of beryllium deuteride cation (BeD⁺) with electrons. We assumed that BeD⁺ is initially in its electronic ground state, X¹Σ⁺, with energies below its dissociation limit. The electron-impact collision processes covered by the present article involve two mechanisms which are treated simultaneously by the MQDT [26]: (*i*) the *direct* process, in which the electron is captured into a doubly excited resonant state BeD^{**} of the neutral system, resulting in two

neutral atomic fragments Be and D or in autoionization,



and (ii) the *indirect* process consisting in the temporary capture of the electron into BeD^* , a singly excited bound Rydberg state, predissociated by BeD^{**} ,



In the MQDT approach, the processes (i) and (ii) result in the total mechanism by quantum interference. As mentioned in Eqs. (6) and (7), the excited neutral system, reached by the electron capture, can autoionize to the initial electronic state of a different vibrational quantum number v_f^+ and then expel an electron to the continuum. Vibrational excitation takes place when $v_f^+ > v_i^+$, while vibrational de-excitation occurs if $v_f^+ < v_i^+$. The quantum defect approach treats the processes represented by Eqs. (6) and (7) as multichannel reactive processes involving the dissociation channels (accounting for the atom-atom scattering) and ionization channels (accounting for the electron-molecular ion scattering). Each ionization channel, for which the collision coordinate is the electron distance r from the molecular ion center, is defined by its threshold, a vibrational level v^+ of the molecular ion ground state and by the angular quantum number l of the incoming or outgoing electron. An ionisation channel is open if its corresponding threshold is situated below the total energy of the system, and closed otherwise. Each closed channels introduce into the calculations a series of Rydberg states BeD^* differing only by the principal quantum number of the external electron [27]. On the other hand, a dissociation channel, having the internuclear distance R as the collision coordinate, relies on an electronically bound state BeD^{**} whose potential energy in the asymptotic limit is situated below the total energy of the system.

Within the Born-Oppenheimer approximation, BeH^+ and BeD^+ ions having the same electronic structure, we used the same set of potential energy curves, electronic couplings [25] and quantum defects as in our previous work on BeH^+ [10, 22], taking care to consider the reduced mass of BeD^+ . Moreover, as the mathematical model is the same, we skip further details and we refer the reader to the previous article [10].

Once the scattering matrix S for the processes DR and VE/VdE are determined, the corresponding global cross sections, as a function of the incident electron kinetic energy ε , are obtained by summation over all relevant symmetries of the system and over the projection of the total electronic angular momentum on the nuclear axes Λ of the resulting partial capture cross sections σ into all the dissociative states d_j of the same symmetry:

$$\sigma_{\text{diss} \leftarrow v_i^+}(\varepsilon) = \frac{\pi}{4\varepsilon} \sum_{\Lambda, \text{sym}} \rho^{\text{sym}, \Lambda} \sum_{l, j} \left| S_{d_j, l v_i^+}^{\Lambda} \right|^2, \quad (8)$$

$$\sigma_{v_f^+ \leftarrow v_i^+}(\varepsilon) = \frac{\pi}{4\varepsilon} \sum_{\Lambda, \text{sym}} \rho^{\text{sym}, \Lambda} \sum_{l, l'} \left| S_{l' v_f^+, l v_i^+}^{\Lambda} - \delta_{l'l} \delta_{v_i^+ v_f^+} \right|^2 \quad (9)$$

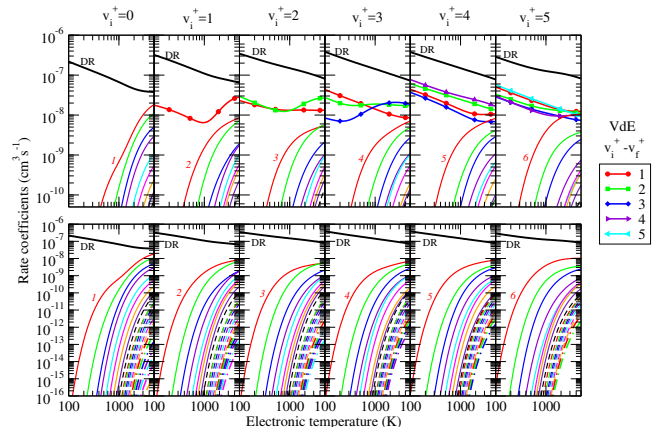


FIG. 1: Dissociative recombination (DR, black line), vibrational excitation (VE, thin lines) and vibrational de-excitation (VdE, symbols and thick lines) rate coefficients of BeD^+ in its electronic ground state for $v_i^+ = 0, \dots, 5$. Upper panels: For each initial vibrational state of BeD^+ , the final vibrational quantum numbers are labeled for de-excitation and for the first one vibrational excitation curve. The remaining unlabeled curves correspond to VE rate coefficients of the ion in the successive increase (in the order) of the vibrational quantum numbers. Lower panels: The same data without those of VdE process, the panels extending the range down to 10^{-16} cm^3/s .

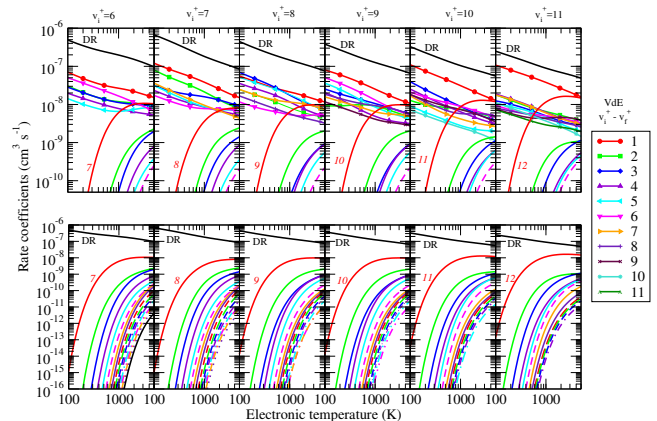


FIG. 2: Same as in Fig. 1 for $v_i^+ = 6, \dots, 11$.

where $\rho^{\text{sym}, \Lambda}$ is the multiplicity ratio between the electronic states of BeD and the electronic states of BeD^+ . In Eq.(9), the vibrational transition occurs *via* the temporarily neutral BeD^* (direct process) or BeD^{**} (indirect process) molecule electronic state. In Eq.(9), l denotes the partial wave of the incident electron and l' that of the outgoing electron. The total state multiplicities of the fragments (D and Be) are those of the BeD molecular state. Notice that the Eqs. (8) and (9) are written in

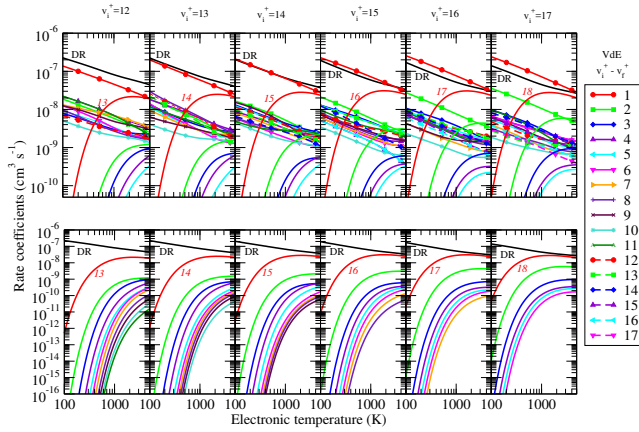


FIG. 3: Same as in Fig. 1 for $v_i^+ = 12, \dots, 17$.

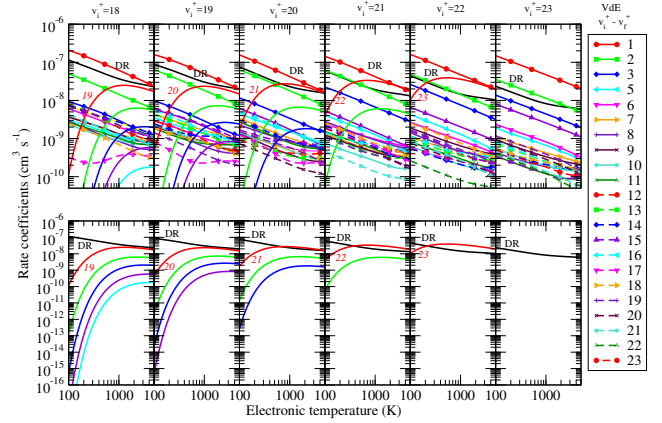


FIG. 4: Same as in Fig. 1 for $v_i^+ = 18, \dots, 23$.

atomic units.

In order to obtain the thermal rate coefficients, we have convoluted the global cross sections with the Maxwellian distribution function for velocities v (related to incident energy of the electrons by $\varepsilon = \frac{1}{2}mv^2$) of the free electrons:

$$\alpha(T) = \frac{8\pi}{\sqrt{m}(2\pi k_B T)^{3/2}} \int_0^{+\infty} \sigma(\varepsilon) \varepsilon \exp(-\varepsilon/k_B T) d\varepsilon, \quad (10)$$

where $\sigma(\varepsilon)$ is the cross sections given by (8) or (9), k_B and T being the Boltzman constant and the absolute temperature respectively.

III. RESULTS

Using the available molecular data shown in Figure 1 of [22] (for more details see as well [25, 28]) - the potential energy curves in a quasi-diabatic representation and electronic Rydberg-valence couplings $5^2\Pi$, $5^2\Sigma^+$ and $1^2\Delta$ states - we have performed calculations corresponding to all vibrational levels (up to $v_i^+ = 23$) of the ground electronic state of the ion. These 24 vibrational levels have been obtained in solving the radial Schroedinger equation by Numerov method, using the potential energy curve of BeH^+ electronic ground state from Ref. [25]. Table I shows the list of vibrational levels of BeD^+ and the values of D_e and D_0 . Notice that these values, as well as some of the potential energy curves and couplings for the neutral, are different from those of Ref. [21] since the molecular data have been obtained using different quantum chemical methods. In the following calculations, the energy of the electron is below to 2.7 eV, this value being only slightly higher than the dissociation threshold D_0 of the ground electronic state of the ion.

Figures 1–4 give the whole ensemble of rate coefficients available for the state-to-state kinetics of BeD^+ . They illustrate the fact that DR dominates for $v_i^+ = 0 - 13$ levels at low electron temperature, while the VdE becomes

v^+	ϵ_{v^+} (eV)	v^+	ϵ_{v^+} (eV)
0	0.000	12	1.920
1	0.194	13	2.031
2	0.380	14	2.135
3	0.564	15	2.232
4	0.742	16	2.321
5	0.914	17	2.401
6	1.079	18	2.473
7	1.238	19	2.535
8	1.391	20	2.585
9	1.537	21	2.623
10	1.674	22	2.655
11	1.802	23	2.678

TABLE I: BeD^+ vibrational levels referred to $v^+ = 0$. The values of dissociating energies are $D_e = 2.794$ eV and $D_0 = 2.682$ eV.

more important than the other processes for initial vibrational states $v_i^+ > 13$. Figure 5 provides a comparison between the DR rate coefficients and the global vibrational transitions rate coefficients - *i.e.* coming from the sum over all the possible final levels. The excitation process competes with DR and VdE above 1000 K only.

The rate coefficients shown in Figs. 1-4 have been fitted by a generalized Arrhenius-type formulas in order to be ready for use in codes for kinetics modelling. The calculated DR rate coefficients of BeD^+ in each of its first 24 vibrational states ($v_i^+ = 0 \dots 23$) have been interpolated under the mathematical form:

$$k_{v_i^+}^{DR}(T_e) = A_{v_i^+} T_e^{\alpha_{v_i^+}} \exp \left[- \sum_{j=1}^7 \frac{B_{v_i^+}(j)}{j T_e^j} \right], \quad (11)$$

over the electron temperature range $100 \leq T_e \leq 5000$ K. The parameters $A_{v_i^+}$, $\alpha_{v_i^+}$ and $B_{v_i^+}(j)$ are listed in the Table II. The calculated VE and VdE rate coefficients of

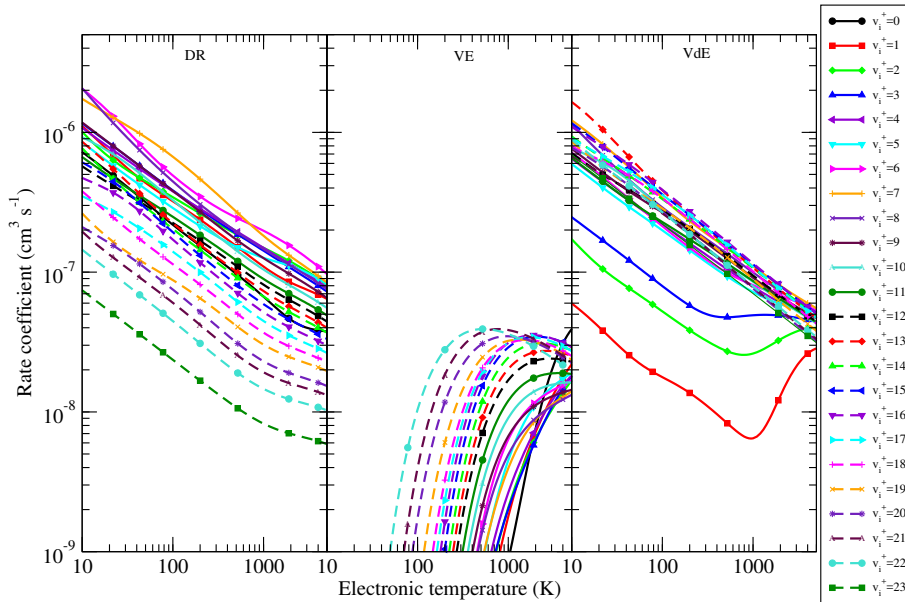


FIG. 5: Dissociative recombination (DR), vibrational excitation (VE) and vibrational de-excitation (VdE) rate coefficients for various initial vibrational states indicated in the legend, those of VE and VdE processes being obtained by sum over all the final states.

BeD⁺ have been interpolated under the form:

$$k_{v_i^+ \rightarrow v_f^+}^{V(d)E}(T_e) = A_{v_i^+ \rightarrow v_f^+} T_e^{\alpha_{v_i^+ \rightarrow v_f^+}} \exp \left[- \sum_{j=1}^7 \frac{B_{v_i^+ \rightarrow v_f^+}(j)}{j T_e^j} \right], \quad (12)$$

over the electron temperature range $300 \leq T_e \leq 5000$ K.

The parameters $A_{v_i^+ \rightarrow v_f^+}$, $\alpha_{v_i^+ \rightarrow v_f^+}$ and $B_{v_i^+ \rightarrow v_f^+}(j)$ are listed in the Table III for the single quantum VE, *i.e.* $v_f^+ = v_i^+ + 1$. The fitted values obtained by Eqs. (11) and (12) depart from the calculated values only of a few percent. The full set of coefficients for DR, VE and VdE are given in the supplementary material of the present article.

IV. CONCLUSIONS

The present paper provides complete set of vibrational resolved rate coefficients for BeD⁺ cation reactive collisions with electrons below to the ion dissociation threshold. In particular, the competition between the vibrational transitions and dissociative recombination processes are illustrated quantitatively. Arrhenius-type formulas are used for fitting the rate coefficients as function of the electron temperature. The rate coefficients are strongly dependent on the initial vibrational level of the molecular ion.

These data are relevant for the modeling of the edge of

the fusion plasma. The higher energy region, where the dissociative excitation process [21, 29] competes the dissociative recombination and the vibrational transitions, as well as similar calculations on BeT⁺, are object of ongoing work.

Acknowledgments

SN is grateful to the project “Projet 1 du Programme CUI: Université du Burundi -VLIR” for the research stay in KULeuven during which the major part of the work has been carried out. VL, JZM, AB and IFS acknowledge the French LabEx EMC³, *via* the projects PicoLIBS (ANR-12-BS05-0011-01) and EMoPlaF, the BIO-ENGINE project and the VIRIDIS-CO2 project (sponsored by the European fund FEDER and the French CPER), the Fédération de Recherche Fusion par Confinement Magnétique - ITER and the European COST Program CM1401 (Our Astrochemical History). JZM is grateful for financial support from Labex SEAM and IDEX-USPC. We are also grateful to the French

Data availability

Upon a reasonable request, the data supporting this article will be provided by the corresponding author.

TABLE II: List of the parameters used in Eq. (11) for the DR rate coefficients of BeD⁺.

v_i^+	$A_{v_i^+}$ ($\text{cm}^3 \cdot \text{s}^{-1} \cdot \text{K}^{-\alpha}$)	$\alpha_{v_i^+}$	$B_{v_i^+(1)}$ ($\times 10^3 \text{ K}$)	$B_{v_i^+(2)}$ ($\times 10^6 \text{ K}^2$)	$B_{v_i^+(3)}$ ($\times 10^9 \text{ K}^3$)	$B_{v_i^+(4)}$ ($\times 10^{11} \text{ K}^4$)	$B_{v_i^+(5)}$ ($\times 10^{14} \text{ K}^5$)	$B_{v_i^+(6)}$ ($\times 10^{15} \text{ K}^6$)	$B_{v_i^+(7)}$ ($\times 10^{17} \text{ K}^7$)
0	0.8974×10^{-09}	0.3841	-2.563	2.470	-1.13	2.766	-0.3713	2.571	-0.7179
1	0.6299×10^{-06}	-0.2688	-0.0219	-0.3068	0.2394	-0.7544	0.1177	-0.9028	0.2710
2	0.1395×10^{-04}	-0.5889	0.7304	-0.7024	0.3170	-0.7705	0.1032	-0.7156	0.2002
3	0.3307×10^{-05}	-0.4462	0.09445	-0.08147	0.03345	-0.07925	0.01074	-0.07665	0.02216
4	0.4349×10^{-05}	-0.4673	0.2376	-0.2605	0.1310	-0.3448	0.04893	-0.3541	0.1023
5	0.2623×10^{-04}	-0.6473	1.421	-1.540	0.7367	-1.848	0.2520	-1.766	0.4973
6	0.3822×10^{-04}	-0.6855	0.7458	-0.5492	0.1993	-0.4139	0.04962	-0.3181	0.08418
7	0.6649×10^{-05}	-0.5080	0.2471	-0.4732	0.2797	-0.7808	0.1134	-0.8287	0.2402
8	0.7614×10^{-05}	-0.5318	0.4697	-0.5195	0.2456	-0.6106	0.08275	-0.5776	0.1623
9	0.6493×10^{-05}	-0.5295	0.5057	-0.6108	0.3022	-0.7682	0.1054	-0.7416	0.2094
10	0.3819×10^{-05}	-0.4877	0.4455	-0.6156	0.3269	-0.8697	0.1230	-0.8836	0.2532
11	0.2883×10^{-05}	-0.4686	0.4699	-0.6798	0.3766	-1.028	0.1479	-1.074	0.3105
12	0.2315×10^{-05}	-0.4563	0.4047	-0.6130	0.3466	-0.9566	0.1385	-1.011	0.2931
13	0.1442×10^{-05}	-0.4155	0.2709	-0.4825	0.2839	-0.8004	0.1174	-0.8643	0.2521
14	0.9694×10^{-06}	-0.3803	0.1729	-0.3907	0.2413	-0.6932	0.1026	-0.7602	0.2226
15	0.7270×10^{-06}	-0.3590	0.1667	-0.4139	0.2543	-0.7253	0.1068	-0.7881	0.2301
16	0.4768×10^{-06}	-0.3232	0.1124	-0.3870	0.2458	-0.7065	0.1042	-0.7692	0.2245
17	0.3339×10^{-06}	-0.2965	0.08587	-0.3909	0.2567	-0.7453	0.1104	-0.8167	0.2387
18	0.2383×10^{-06}	-0.2735	0.1221	-0.4597	0.2953	-0.8485	0.1250	-0.9205	0.2683
19	0.1868×10^{-06}	-0.2609	0.1973	-0.5555	0.3423	-0.9644	0.1404	-1.025	0.2974
20	0.1332×10^{-06}	-0.2495	0.2343	-0.6118	0.3644	-1.009	0.1454	-1.056	0.3048
21	0.1114×10^{-06}	-0.2452	0.2826	-0.6493	0.3776	-1.035	0.1486	-1.076	0.3102
22	0.8079×10^{-07}	-0.2366	0.2937	-0.6480	0.3747	-1.027	0.1475	-1.069	0.3084
23	0.4801×10^{-07}	-0.2398	0.3455	-0.7133	0.4152	-1.148	0.1659	-1.208	0.3498

TABLE III: List of the parameters used in Eq. (12) for the monoquantic VE, $v_i^+ \rightarrow v_f^+ = v_i^+ + 1$, rate coefficients of BeD⁺.

v_i^+	$A_{v_i^+ \rightarrow v_f^+}$ ($\text{cm}^3 \cdot \text{s}^{-1} \cdot \text{K}^{-\alpha}$)	$\alpha_{v_i^+ \rightarrow v_f^+}$	$B_{v_i^+ \rightarrow v_f^+(1)}$ ($\times 10^4 \text{ K}$)	$B_{v_i^+ \rightarrow v_f^+(2)}$ ($\times 10^7 \text{ K}^2$)	$B_{v_i^+ \rightarrow v_f^+(3)}$ ($\times 10^{10} \text{ K}^3$)	$B_{v_i^+ \rightarrow v_f^+(4)}$ ($\times 10^{13} \text{ K}^4$)	$B_{v_i^+ \rightarrow v_f^+(5)}$ ($\times 10^{15} \text{ K}^5$)	$B_{v_i^+ \rightarrow v_f^+(6)}$ ($\times 10^{18} \text{ K}^6$)	$B_{v_i^+ \rightarrow v_f^+(7)}$ ($\times 10^{19} \text{ K}^7$)
0	$0.232 \times 10^{+02}$	-2.10	1.68	-1.56	-0.611	1.73	-10.1	2.51	-23.0
1	0.395×10^{-09}	0.361	-0.0592	0.698	-0.787	0.442	-1.28	0.176	-0.830
2	0.156×10^{-11}	0.887	-0.423	1.26	-1.35	0.833	-2.94	0.551	-4.24
3	0.240×10^{-06}	-0.294	0.638	-1.58	2.16	-1.50	5.67	-1.10	8.67
4	0.109×10^{-07}	0.0162	0.249	-0.457	0.739	-0.555	2.18	-0.439	3.53
5	0.432×10^{-08}	0.0776	-0.205	1.13	-1.44	0.960	-3.51	0.669	-5.19
6	0.517×10^{-08}	0.0507	-0.211	0.892	-1.0	0.639	-2.29	0.435	-3.36
7	0.753×10^{-08}	-0.00187	-0.107	0.714	-0.824	0.509	-1.75	0.318	-2.36
8	0.128×10^{-07}	-0.0677	-0.0679	0.444	-0.448	0.262	-0.889	0.160	-1.19
9	0.220×10^{-06}	-0.353	0.0627	0.160	-0.141	0.0746	-0.234	0.0402	-0.290
10	0.143×10^{-05}	-0.530	0.138	0.00943	0.0135	-0.0209	0.107	-0.0249	0.220
11	0.380×10^{-05}	-0.613	0.172	-0.0627	0.0732	-0.0503	0.195	-0.0394	0.321
12	0.850×10^{-05}	-0.673	0.196	-0.135	0.151	-0.0976	0.358	-0.0693	0.547
13	0.144×10^{-04}	-0.718	0.216	-0.203	0.230	-0.148	0.542	-0.104	0.824
14	0.129×10^{-04}	-0.698	0.192	-0.167	0.184	-0.114	0.404	-0.0755	0.578
15	0.160×10^{-04}	-0.719	0.193	-0.204	0.237	-0.153	0.556	-0.106	0.827
16	0.153×10^{-04}	-0.723	0.181	-0.207	0.247	-0.161	0.591	-0.113	0.893
17	0.103×10^{-04}	-0.700	0.153	-0.162	0.189	-0.121	0.434	-0.0817	0.630
18	0.784×10^{-05}	-0.691	0.137	-0.150	0.176	-0.113	0.405	-0.0765	0.589
19	0.401×10^{-05}	-0.638	0.0942	-0.0839	0.0939	-0.0576	0.199	-0.0365	0.276
20	0.323×10^{-05}	-0.609	0.0779	-0.0786	0.0904	-0.0574	0.205	-0.0387	0.298
21	0.273×10^{-05}	-0.573	0.0600	-0.0489	0.0528	-0.0319	0.109	-0.0200	0.150
22	0.221×10^{-05}	-0.545	0.0446	-0.0367	0.0403	-0.025	0.0878	-0.0162	0.123

- [1] A. W. Kleyn, N. J. Lopes Cardozo and U. Samm, Phys. Chem. Chem. Phys. 8(2006) 1761–1774.
[2] G. Duxbury, M.F. Stamp and H.P. Summers, Plasma Phys. Control. Fusion 40 361-370 (1998).
[3] S. Brezinsek, M.F. Stamp, D. Nishijima, D. Borodin, S. Devaux, K. Krieger, S. Marsen, M. OMullane, C. Bjoerkas, A. Kirschner and JET EFDA contributors, Nucl.

- Fusion 54 (2014) 103001 (11pp).
[4] S. Brezinsek, A. Widdowson, M. Mayer, V. Philipps, P. Baron-Wiechec, J.W. Coenen, K. Heinola, A. Huber, J. Likonen, P. Petersson, M. Rubel, M.F. Stamp, D. Borodin, J.P. Coad, A.G. Carrasco, A. Kirschner, S. Krat, K. Krieger, B. Lipschultz, Ch. Linsmeier, G.F. Matthews, K. Schmid and JET contributors, Nucl. Fu-

- sion 55 (2015) 063021 (10pp).
- [5] J.W. Coenen, M. Sertoli, S. Brezinsek, I. Coffey, R. Dux, C. Giroud, M. Groth, A. Huber, D. Ivanova, K. Krieger, K. Lawson, S. Marsen, A. Meigs, R. Neu, T. Puetterich, G.J. van Rooij, M.F. Stamp and JET-EFDA Contributors, Nucl. Fusion 53 (2013) 073043.
- [6] G.F. Matthews, JET EFDA Contributors, the ASDEX-Upgrade Team, J. Nucl. Mater. 438 (2013) S2-S10.
- [7] S. Brezinsek, T. Loarer, V. Philipps, H.G. Esser, S. Grünhagen, R. Smith, R. Felton, J. Banks, P. Belo, A. Boboc, J. Bucalossi, M. Clever, J.W. Coenen, I. Coffey, S. Devaux, D. Douai, M. Freisinger, D. Frigione, M. Groth, A. Huber, J. Hobirk, S. Jachmich, S. Knipe, K. Krieger, U. Kruezi, S. Marsen, G.F. Matthews, A.G. Meigs, F. Nave, I. Nunes, R. Neu, J. Roth, M.F. Stamp, S. Vartanian, U. Samm and JET EFDA contributors, Nucl. Fusion 53 (2013) 083023 (13pp).
- [8] V. Kh. Alimov, Physica Scripta. Vol. T108 (2004), 46–56.
- [9] O. Motapon, S. Niyonzima, K. Chakrabarti, J.Zs. Mezei, D. Backodissa, S. Ilie, M.D. Epee Epee, B. Peres, M. Lanza, T. Tchakoua, N. Pop, F. Argoubi, M. Telmini, O. Dulieu, A. Bultel, J. Robert, Å. Larson, A.E. Orel and I.F. Schneider, EPJ Web of Conferences 84 (2015) 02003
- [10] S. Niyonzima, S. Ilie, N. Pop, J. Zs. Mezei, K. Chakrabarti, V. Morel, B. Peres, D.A. Little, K. Has-souni, A. Larson, A.E. Orel, D. Benredjem, A. Bultel, J. Tennyson, D. Reiter, I.F. Schneider, Atomic Data and Nuclear Data Tables, 115-116 (2017), 287 - 308
- [11] K. Krieger, S. Brezinsek, M. Reinelt, S.W. Lisgo, J.W. Coenen, S. Jachmich, S. Marsen, A. Meigs, G. van Rooij, M. Stamp, O. van Hoey, D. Ivanova, T. Loarer, V. Philipps, and JET EFDA contributors, J. Nucl. Mater. 438 (2013) S262–S266.
- [12] D. Nishijima, R. P. Doerner, M. J. Baldwin, G. De Temmerman and E. M. Hollmann, Plasma Phys. Control. Fusion 50 (2008) 125007.
- [13] D. Darby-Lewis, J. Tennyson, K. D. Lawson, S. N. Yurchenko, M. F Stamp, A. Shaw and JET Contributors, J. Phys. B: At. Mol. Opt. Phys. (submitted).
- [14] R.P. Doerner, M.J. Baldwin, D. Buchenauer, G. De Temmerman, D. Nishijima, J. Nucl. Mater.390-391(2009) 681.
- [15] J.A. Coxon and R. Colin, J. Mol. Spectrosc. 181, 215-223 (1997).
- [16] P. G. Koontz, Phys. Rev. 48 (1935) 707-713.
- [17] G.M. McCracken, M.F. Stamp, R.D. Monk, A.G. Meigs, J. Lingertat, R. Prentice, A. Starling, R.J. Smith and A. Tabasso, Nucl. Fus. 38(1998) 619.
- [18] S. I. Krashennikov, Physica. Scripta (2002) T96, 7-15.
- [19] R. Celiberto, R. K. Janev, A. Laricchiuta, M. Capitelli, J. M. Wadehra and D. E. Atoms, Atom. Data Nucl. Data Tabl. 77 (2001) 161–213.
- [20] R. Celiberto, R. K. Janev, and D. Reiter, Plasma Phys. Control. Fusion 54 (2012) 035012.
- [21] V Laporta, K Chakrabarti, R Celiberto, R K Janev, J Zs Mezei, S Niyonzima, J Tennyson, and I F Schneider. *Plasma Physics and Controlled Fusion*, 59(4):045008, 2017.
- [22] S. Niyonzima, F. Lique, K. Chakrabarti, Å. Larson , A. E. Orel, and I. F. Schneider, Phys. Rev. A 87 (2013) 022713.
- [23] D. Darby-Lewis, Z. Masin and J. Tennyson, J. Phys. B: At. Mol. Opt. Phys., 50 (2017) 175201.
- [24] I. F. Schneider, O. Dulieu, and J. Robert (editors), EPJ Web of Conferences 84 (2015) (Proceedings of the 9th International Conference 'Dissociative Recombination: Theory, Experiment and Applications', Paris, July 7-12 2013).
- [25] J. B. Roos , M. Larsson, Å. Larson, and A. E. Orel, Phys. Rev. A 80 (2009) 012501.
- [26] A. Giusti, J. Phys. B 13 (1980) 3867.
- [27] Schneider I F, Dulieu O, Giusti-Suzor A, and Roueff E 1994, Astrophys. J. **424**, 983.
- [28] C. Strömholm, I. F. Schneider, G. Sundström, L. Carata, H. Danared, S. Datz, O. Dulieu, A. Källberg, M. af Ug-glas, X. Urbain, V. Zengin, A. Suzor-Weiner, and M. Larson, Phys. Rev. A 52 (1995) R4320.
- [29] K. Chakrabarti, D. R. Backodissa-Kiminou, N. Pop, J. Zs. Mezei, O. Motapon, F. Lique, O. Dulieu, A. Wolf and I. F. Schneider, Phys. Rev. A **87** (2013) 022702.